Biochimica et Biophysica Acta 1787 (2009) 617–625

Contents lists available at ScienceDirect

Biochimica et Biophysica Acta

journal homepage: www.elsevier.com/locate/bbabio

Monitoring the redox and protonation dependent contributions of cardiolipin in electrochemically induced FTIR difference spectra of the cytochrome bc_1 complex from yeast

Ruth Hielscher [a], Tina Wenz [b,1], Carola Hunte [b,2], Petra Hellwig [a,*]

[a] Laboratoire vibrationnelle et électrochimie des biomolécules, Institut de Chimie, UMR 7177, CNRS, Université de Strasbourg, 1 rue Blaise Pascal, F-67070 Strasbourg, France
[b] Max-Planck-Institute of Biophysics, Department of Molecular Membrane Biology, Max-von- Laue-Straβe 3, D-60438 Frankfurt am Main, Germany

ARTICLE INFO

Article history:
Received 1 December 2008
Received in revised form 12 January 2009
Accepted 12 January 2009
Available online 20 January 2009

Keywords:
FTIR spectroscopy
Low frequency region
Phospholipids
BC1 complex
Cardiolipin
Electrochemistry

ABSTRACT

Biochemical studies have shown that cardiolipin is essential for the integrity and activity of the cytochrome bc_1 complex and many other membrane proteins. Recently the direct involvement of a bound cardiolipin molecule (CL) for proton uptake at center N, the site of quinone reduction, was suggested on the basis of a crystallographic study. In the study presented here, we probe the low frequency infrared spectroscopy region as a technique suitable to detect the involvement of the lipids in redox induced reactions of the protein. First the individual infrared spectroscopic features of lipids, typically present in the yeast membrane, have been monitored for different pH values in micelles and vesicles. The pK_a values for cardiolipin molecule have been observed at 4.7 ± 0.3 and 7.9 ± 1.3, respectively. Lipid contributions in the electrochemically induced FTIR spectra of the bc_1 complex from yeast have been identified by comparing the spectra of the as isolated form, with samples where the lipids were digested by lipase-A_2. Overall, a noteworthy perturbation in the spectral region typical for the protein backbone can be reported. Interestingly, signals at 1159, 1113, 1039 and 980 cm^{-1} have shifted, indicating the perturbation of the protonation state of cardiolipin coupled to the reduction of the hemes. Additional shifts are found and are proposed to reflect lipids reorganizing due to a change in their direct environment upon the redox reaction of the hemes. In addition a small shift in the alpha band from 559 to 556 nm can be seen after lipid depletion, reflecting the interaction with heme b_H and heme *c*. Thus, our work highlights the role of lipids in enzyme reactivity and structure.

1. Introduction

Reaction induced FTIR difference spectroscopy allows monitoring at molecular level the reorganization within a molecule, protein or any other material upon the induced reaction. On this basis it is possible to contribute to the understanding of mechanisms in molecular bioenergetics. The technique is especially successful in characterizing the protonation state of individual amino acid side chains in the mid infrared, with a special focus on protonated aspartic and glutamic acid side chains and quinones (as reviewed among many other studies in [1,2]). The rich signal structures in the low frequency domain, the called finger print area, include small but specific signals of side chains. Between 1400 and 800 cm^{-1} for example contributions from quinols [3], histidines [4,5] and the hemes [6,7] can be depicted in the data obtained from a reaction induced FTIR difference spectrum. In the far infrared region (<800 cm^{-1}) the contributions of metal–ligand vibrations [8,9] and of the hydrogen bonding collective motions can be probed [10]. These low frequency modes also involve the contributions from water chains in the protein and several THz time domain approaches study the time resolved reorganization of water within an induced reaction like for example protein refolding [11]. The spectroscopic characterization of low frequency signals may lead to an understanding of the protein dynamics that give rise to protein function, including ligand accommodation, electron and proton transfer.

In this manuscript we present on the use of this spectral region for the study on the role of phospholipids, bound within the protein structure and, importantly, reorganizing during the redox reaction of the protein. The infrared spectroscopic properties of lipids and membranes are well known from previous studies by several groups [12–17]. Infrared spectroscopic studies on lipid reorganization, mostly of phospholipid phase transitions in model lipid bilayers investigated in a temperature dependent manner, have provided insight to features of the different structures and the behavior of individual vibrational

Abbreviations: FTIR, Fourier-transform infrared; CL, cardiolipin, bisphosphatidylglycerol; PC, phosphatidylcholine; PE, phosphatidylethanolamine; PG, phosphatidylglycerol; UV–vis, ultraviolet–visible; Tris, tris-hydroxymethylaminoethane; cytochrome bc_1 complex, ubiquinone:cytochrome *c* oxidoreductase

* Corresponding author.
E-mail address: hellwig@chimie.u-strasbg.fr (P. Hellwig).
[1] Current address: Miller School of Medicine, Department of Neurology, Lois Pope Life Center R. 3.01, University of Miami, 1095 NW 14th Terrace, Miami, FL 33136, USA.
[2] Current address: Institute of Membrane and Systems Biology, University of Leeds, Leeds LS2 9JT, UK.

0005-2728/$ – see front matter © 2009 Elsevier B.V. All rights reserved.
doi:10.1016/j.bbabio.2009.01.006

modes in model and natural membranes [15,18,19]. Furthermore reports describing the effect of lipids on secondary structure arrangements on the basis of amide I band deconvolutions are available [20].

During the past few years, a number of structures of integral membrane proteins at high resolution have emerged. Some of them show protein-associated phospholipid molecules [21–23] (and see reviews in Ref. [24–26]). Biochemical studies have shown that phospholipids are essential for the activity of several membrane proteins, but the role of structurally resolved phospholipids has not been clarified yet. The effect of Rhodopsin activation on specific neighboring phospholipids was demonstrated by FTIR spectroscopy and signals in the spectral region characteristic for ester groups were reported [27–30]. This indicates that in the spectral region, were typically contributions from protonated aspartic and glutamic acid residues are found and discussed in reaction induced FTIR difference spectra [31,32], contributions from lipids may be involved as well. Similarly we could show in a recent study, that the reactivation of complex I with lipids affects the spectral range characteristic for the C=O vibration [33]. Evidently bound phospholipids may influence and even contribute to reaction induced FTIR difference spectra.

The Ubiquinol:cytochrome *c* oxidoreductase (cytochrome bc_1 complex; complex III) contains such specifically bound lipids [22,25]. The enzyme is one of the fundamental components of respiratory electron transfer chains, located in the inner mitochondrial or bacterial cytoplasmic membrane. It couples the electron transfer from ubiquinol to cytochrome *c* to translocation of protons across the membrane [34]. As a minimum requirement, all bc_1 complexes contain three catalytic subunits: cytochrome *b* with two *b*-type hemes (cytochrome b_L and b_H), cytochrome c_1 with a covalently bound *c*-type heme, and the Rieske iron sulfur protein with a [2Fe–2S] cluster [35–37]. Digestion of tightly bound phospholipids inactivates the cytochrome bc_1 complex and reactivation depends on addition of cardiolipin [38]. For example, phospholipase A_2 cleaves the middle (*sn*-2) ester bond of phospholipids [39] and is useful for digestion of tightly bound phospholipids from the enzymes [38,40].

The crystal structure from the cytochrome bc_1 complex from the yeast *Saccharomyces cerevisiae* was determined at 2.3 Å resolution [41]. Two cardiolipin molecules have been identified in the structure of the yeast cytochrome bc_1 complex [22,25]. It is proposed that a tightly bound cardiolipin molecule participates directly or indirectly in proton uptake at center N, the site of quinone reduction and to be of importance for the stability of the catalytic site [22]. Elucidating the function of specifically bound phospholipids molecules is important to fully understand the molecular mechanism of membrane proteins.

The presented study consists of two parts. First we present the pH dependent behavior of cardiolipin vibrational modes in vesicles and micelles and compare the spectral feature as well as further lipids from the mitochondrial membrane. Vibrational modes are depicted, which might be expected in a protonation event within the enzyme. In the second part of the study, electrochemically induced FTIR difference spectra of the bc_1 complex from yeast, prepared with different lipid content, are presented that characterize signals specific for cardiolipin and other phospholipids.

2. Materials and methods

2.1. Liposome preparation

The liposomes were prepared by sonification of lipids resuspended for each of the pH values in the respective 20 mM buffer (glycine/HCl, pH 2; glycine/HCl, pH 3; sodium acetate, pH 4; sodium acetate, pH 5; potassium phosphate, pH 6; potassium phosphate, pH 7; Tris/HCl, pH 8 and glycine/NaOH, pH 9) supplemented with sodium cholate (1% w/v). The lipid mixture contains 400 µg cardiolipin (CL), 900 µg phosphatidylcholine (PC) and 700 µg phosphatidylethanolamine (PE) per 100 µl and corresponds to the ratio of the mitochondrial inner membrane in *Saccharomyces cerevisiae*. For the CL vesicles a concentration of 20 mg per ml was used. Phosphatidylglycerol (PG), PC and PE vesicles (20 mg/ml each) (all purchased from Sigma-Aldrich) were prepared as well as a mix of PC and PE with a ratio of 11: 9 mg/ml. The detergent was removed by incubation of the solution with biobeads (~50 mg/ml) for 6–12 h at 4 °C. Biobeads were removed by centrifugation. The vesicle solution was used without further purification. The solution was used fresh or stored for up to one week at 4 °C.

Micelles have been obtained from cardiolipin and phosphatidylglycerol (Sigma-Aldrich). The samples were used without further purification and dissolved in water, ethanol or ethanol-d_1 (Sigma-Aldrich) at room temperature.

2.2. Cytochrome bc_1 complex purification

The wild-type *Saccharomyces cerevisiae* strain was grown in YPG medium and harvested at late logarithmic phase. Mitochondrial membranes and cytochrome bc_1 preparation were carried out as described before [42]. Briefly, membranes were prepared of a 60% (w/v) cell suspension in a cell mill equipped with glass beads. Cell debris was separated at 5000 *g* for 45 min and membranes were collected from the supernatant by ultracentrifugation at 150,000 *g* for 60 min. Cytochrome bc_1 was solubilized with n-dodecyl-β-D-maltopyranoside (LM) and purified via two consecutive DEAE anion exchange chromatographic steps. The detergent was exchanged to 0.05% (w/v) n-undecyl-β-D-maltopyranoside (UM) with the second DEAE chromatography step. Extinction coefficients of 17. 5 mM^{-1} cm^{-1} for *c*-type heme (553–540 nm, ascorbate/ferricyanide) and 25. 6 mM^{-1} cm^{-1} for *b*-type hemes (562–575 nm, dithionite/ferricyanide) were used for redox-spectroscopic quantification of cytochrome bc_1.

2.3. Lipid free bc_1 complex

Purified cytochrome bc_1 was diluted to 15 µM in 2 mM $CaCl_2$, 50 mM Tris–HCl, pH 7.4, 250 mM NaCl, 0.05% UM. The enzyme was delipidated by incubation with 66 U/ml phospholipase A_2 (Sigma-Aldrich) for 1 h at room temperature. Delipidation was stopped by addition of 10 mM EDTA. For relipidation, phospholipids (asolecthin, cardiolipin or a mixture of asolecthin/cardiolipin) were added from a 2% (w/v) stock solution to a final concentration of 0.01% [43]. Turnover experiments were performed for the wild type and the lipid free complex [43].

2.4. Spectroelectrochemistry in the infrared and the visible spectral range

FTIR spectra were obtained on a modified Bruker IFS 25 spectrometer. Absorbance spectra were measured for liposomes and micelle films on AgCl and BaF_2 windows. The spectroelectrochemical cell for the UV/vis and infrared was used as previously reported [44] and the redox induced FTIR difference spectra of the cytochrome bc_1 complex were recorded and processed as previously described [45,46] except for the window material. BaF_2 windows allowed accessing the spectral range down to 800 cm^{-1}. Potentials were measured with an Ag/AgCl/3 M KCl reference electrode and are quoted in reference to the standard hydrogen electrode (pH 7). The full potential step comprises −0.29 to 0.71 V which contains the fully oxidized and the fully reduced form. The redox FTIR and the visible difference spectra are almost perfectly symmetrical.

2.5. Determination of pK values

The p*K* values of the cardiolipin vesicles were determined from the normalized FTIR absorbance spectra (1736 cm^{-1}) at various pH steps. The data was evaluated for the υ(C=O) vibrational modes at 1749 and 1712 cm^{-1} as well as for the υ(PO_3^{2-}) vibrational modes at 955, 978

and 993 cm^{-1}. For the calculation of the two pK_a values we used the Henderson Hasselbach equation. The curves were fitted with the program Origin 5.0 (OriginLab Corporation, Northampton).

3. Results

3.1. Model compound studies on lipids

3.1.1. Infrared absorbance spectra of cardiolipin

Infrared spectra of lipids have been studied for many decades and the infrared spectroscopic properties are known to be easily influenced by the degree of hydration, the structural arrangement, specific hydrogen bonding interactions or protonation states [13,14,47,48]. For a clearer analysis of the contributions expected for the cardiolipin in the yeast cytochrome bc_1 we first studied these effects with cardiolipin alone.

Fig. 1 shows the absorbance spectra of cardiolipin micelles (A) in direct comparison to vesicles (B) at pH 7–7.3. Three major regions can be distinguished in spectra of cardiolipin [14]. Between 3100 cm^{-1} and 2900 cm^{-1} the CH_2 vibrations dominate the data. At 1740–1710 cm^{-1} ν(C=O) vibrational modes are expected, the exact position depending on the hydrogen bonding environment. In the micelles the C=O ester group is observed at 1739 cm^{-1} and a shoulder arises at 1720 cm^{-1} in the vesicle, indicating the structural rearrangement in the direct vicinity of the group. This signal was previously studied [13,49]. The strong peak between 1464 and 1471 cm^{-1} can be attributed to a δ (CH_2) deformation mode [50,51]. Between 1400 and 1150 cm^{-1} the γ (CH_2) wagging or so called Snyder CH_2 wagging progressions vibrations are present. Vibrations associated with the wagging motions of a finite methylene chain have been related to coupled oscillators [50] and are found for the cardiolipin vesicles studied here (Fig. 1B). They are a qualitative index of the chain conformation [52,53] and diagnostic for the all trans-conformation.

Contributions for the phosphate groups are found between 1250 and 840 cm^{-1} [12,15,19,54] and include symmetric and asymmetric vibration of the PO groups and the CO–PO functional groups. Computational calculated infrared spectra of phosphate ions in aqueous solution underline these assignments [55]. It was shown, that the hydration of the studied film influences the exact position of the phosphate modes, and that the position is found at higher wavenumbers, if the degree of hydration is low [49,56,57]. The detailed band assignments based on the well established infrared data on lipids and membranes by several groups are summarized in Table 1.

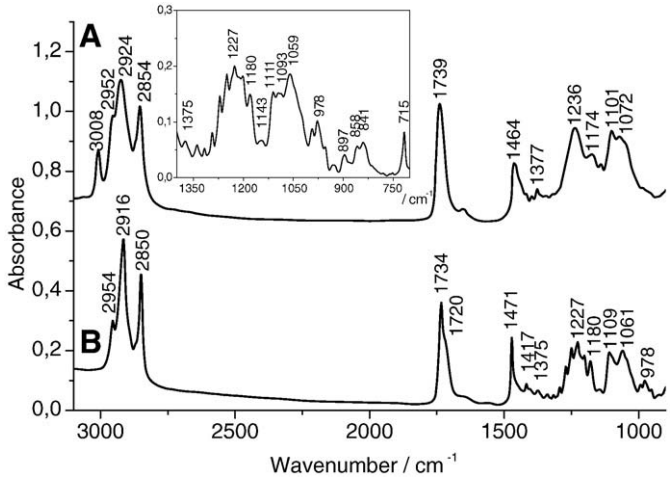

Fig. 1. Infrared absorbance spectra of cardiolipin micelle (A) at pH 7 in direct comparison to cardiolipin as vesicle (B) at pH 7.3 in the full spectral range from 4000 to 900 cm^{-1}. The inset shows the lower frequency region till 700 cm^{-1} where important vibrations from the phosphate group are expected.

Table 1
Tentative assignments of the vibrational modes in the infrared absorbance spectra from cardiolipin and mixed lipids (cardiolipin (CL), phosphatidylcholine (PC) and phoshatidylethanolamine (PE))

Band position/cm^{-1}	Assignments		Comment	Ref.
3008	υ(OH)	P–OH	CL micelle	a,d
2952/2954	$\upsilon_{as}(CH_3)$	C–CH_3		a,c,d
2924/2916	$\upsilon_{as}(CH_2)$	–$(CH_2)_n$–		a,c,d
2870	$\upsilon_s(CH_3)$	C–CH_3		a,c,d
2854/2850	$\upsilon_s(CH_2)$	–$(CH_2)_n$–		a,c,d
1739	υ(C=O)	–CH_2–COOR		a,b,c,d,e
1734	υ_s(C=O)			a,b,c,d,e
1720	υ_{as}(C=O)			a,b,c,d,e
1550	$\delta_{as}(CH_3^+)$	N^+–$(CH_3)_3$	PC/PE	a,d
	$\delta_{as}(NH_3^+)_{twist}$	RNH_3^+	PC/PE	a,d
1471/1464	δ $(CH_2)_{scissor}$	–$(CH_2)_n$–		a,c,d,f,g
1417	δ (CH_2)	–CH_2–COOR	α-methylene	a,c,d,f,g
1377/1375	$\delta_s(CH_3)$	C–CH_3		a,c,d
1400–1180	γ $(CH_2)_{wag}$	–$(CH_2)_n$–	progression bands/CL liposome	a,c,d,f,g
1236/1227	$\upsilon_{as}(PO_2^-)$	RO–PO_2^-–OR′		a,c,d
1227	$\upsilon_{as}(PO_2^-)$	RO–PO_2^-–OR′	potential CL marker	a,c,d
1180/1174	υ_{as}(CO–O–C)	R–COO–R′		a,c,d
1176	υ_{as}(CO–O–C)	R–COO–R′	potential CL marker	a,c,d
1101/1093	$\upsilon_s(PO_2^-)$	RO–PO_2^-–OR′		a,c,d
1088	$\upsilon_s(PO_2^-)$	RO–PO_2^-–OR′	potential CL marker	a,c,d
1072/1061	υ_s(POC)	PO–C		a,c,d
1050	υ_s(POC)	PO–C	potential CL marker	a,c,d
978	$\upsilon(PO_3^{2-})$			a,d
972	υ_s(C–N^+–C)	R–N^+–$(CH_3)_3$	PC/PE	a,d
897	γ (CH_2)	–$(CH_2)_n$–		f,g
858/841	υ(PO)	P–O		a,d
800–700	γ $(CH_2)_{rock/twist}$	–$(CH_2)_n$–	progression bands/CL liposome	f,g
715	γ $(CH_2)_{rock/twist}$	–$(CH_2)_n$–		f,g

Ref.: a: Mantsch et al. [12], b: Blume et al. [13], c: Hübner et al. [14], d: Mantsch and McElhaney [15], f: Snyder [50], g: Snyder and Schachtschneider [51].

3.1.2. pK_a value determination for cardiolipin

In order to depict the pH dependent vibrational modes and signals for the protonation state of the different phosphate groups, the absorbance spectra of the cardiolipin at different pH values have been obtained. Two pH dependent transitions can be expected for the dianionic CL (Fig. 2C). Fig. 2 shows the infrared absorbance spectra of cardiolipin at pH 2–9 in 1 pH unit steps (A). Clearly the change in protonation state induces shifts of nearly all vibrational modes. This can be attributed to the change in protonation state at the phosphate groups that corroborate with structural rearrangements. The Snyder modes of the CH_2 groups are essentially negligible at pH <5, indicating that the side chains are not in the all-trans mode. The ν(C=O) vibration shifts from 1739 cm^{-1} at acidic pH to a split mode at 1736 and 1712 cm^{-1} at pH 9 indicating the presence of a stronger hydrogen bonding to one of the C=O groups.

The difference spectra obtained by the subtraction of the spectra at pH 9–pH 6 and pH 2–pH 6 respectively, seen in Fig. 2B, directly reflect the two protonation steps of the phosphate groups. The sharp peaks in the difference spectrum for the step from pH 2–pH 6 result from shifts of the weaker γ (CH_2) Snyder vibrations. The first protonation event induces a shift of the mode from 952 cm^{-1} to 1032 and 1190 cm^{-1}. The second protonation event at a pH higher than 6, shifts signals from 1190 and 1103 cm^{-1} to 944 cm^{-1}.

On the basis of the shifts observed, we have determined the pK values of cardiolipin. Fig. 3 shows the enlarged view of the pH dependent variations for the absorbance spectra of cardiolipin from pH 2 to pH 9: i.e. of the ν(C=O) vibration at 1712 and 1749 cm^{-1} (A) as well as of the $\nu(PO_3^{2-})$ modes at 955, 978 and 993 cm^{-1} (B). In Fig. 3C the pH dependent curve for the peak position at 955 cm^{-1} is seen. A pK_a value of 4.7 ± 0.3 was found for the first protonation step, by fitting the pH dependence of several modes (see materials and methods).

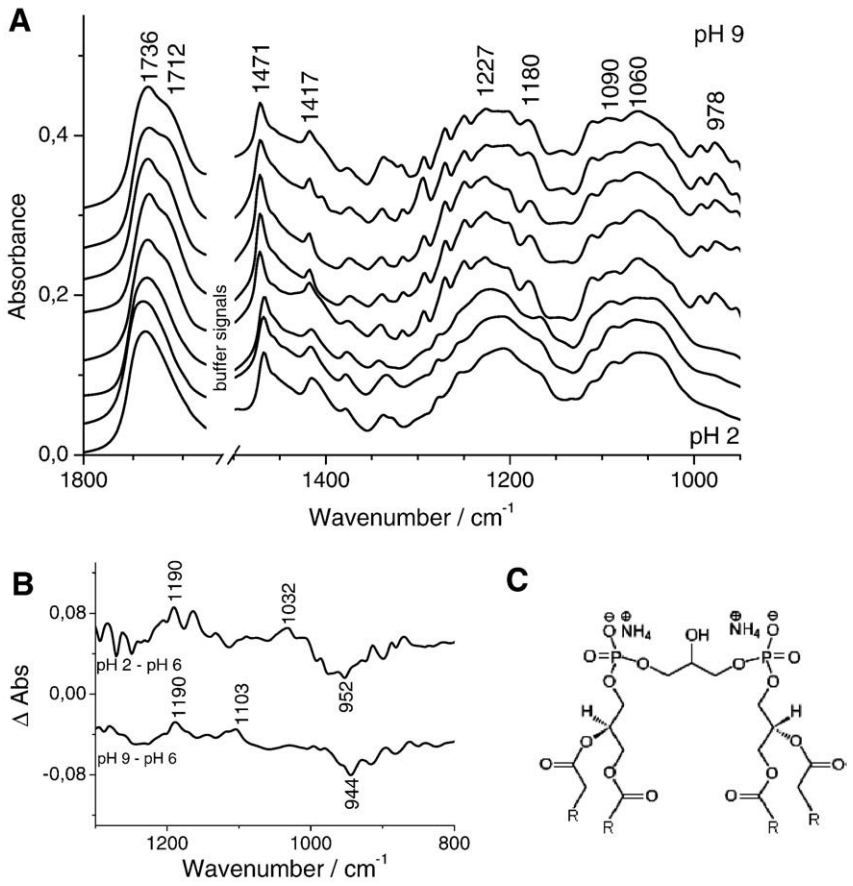

Fig. 2. Infrared absorbance spectra of cardiolipin vesicles at pH 2–pH 9 in steps of 1 pH unit (for buffers see Materials and methods) (A) from 1800 to 900 cm^{-1} and the difference spectra (B) obtained by the subtraction of the spectra at pH 9–pH 6 and pH 2–pH 6, respectively (C) shows the cardiolipin structure.

The second pH dependent change, that indicates the second deprotonation, is found at 7.9 ± 1.3. Due to the complex signal structure below the Snyder modes, a precise determination remains difficult. Similarly, Kates et al. [58] published two pK_a values of cardiolipin at 2.8 and the second at 7.5. Haines and Dencher [59] have proposed a closed structure of the head group, the strong hydrogen bonding inducing this high pK value. It is unlikely to find this ring like structure stabilized in the protein due to steric constraints. Based on the strong influence of the hydrogen bonds stabilizing the molecule, on the pK_a value observable, the pK_a values for the protein bound cardiolipin is not predictable.

3.1.3. Cardiolipin marker band in mixed lipids

In order to find a possible cardiolipin markers, vesicles of CL:PC:PE as similarly found in the mitochondrial membrane, have been studied for the same series of pH values. Fig. 4 shows the infrared absorbance spectra of the mixed lipids at selected pH values. The inset shows the pH dependent variation of the PO modes in the region between 1300 and 950 cm^{-1}.

The contributions of the different lipids are summarized in Table 1. The clearest marker for cardiolipin can be found at 1227, 1176, 1088 and 1050 cm^{-1} from the PO stretch and other head group vibrations, whereas the modes between 1530 and 1400 cm^{-1} are typical for ethanolamine and choline NH_3 and NCH_3 vibrations (see Table 1).

In the spectra of the mixed lipids shown in Fig. 4, a more complex pH dependency is found, due to the high number of phosphate groups, which participate in the spectra. The shifts of the $\nu_{as}(PO_2^-)$ modes from 1227 cm^{-1} at pH 2 and pH 3 to 1238 cm^{-1} at pH 5 and to 1230 cm^{-1} at pH 8 as well as the variation of the signal at 1168 cm^{-1} for the COH stretch vibration from the head group are indicated difference pK_a values of the mixed lipids.

In order to clearly distinguish the pK_a values of the individual components, isotope labeling experiments will be necessary.

3.2. Electrochemically induced FTIR difference spectra

3.2.1. Redox induced FTIR difference spectra in the absence of cardiolipin

The electrochemically induced FTIR difference spectra of proteins include signals that derive from reorganizations of the protein upon the induced redox reaction and coupled protonation events. In addition, the spectra may contain contributions from the cofactors, from lipids that reorganize or protonate upon the redox reaction [33] and protonation events of the buffer.

Fig. 5 shows the oxidized-minus-reduced FTIR difference spectra of the purified yeast cytochrome bc_1 complex as isolated (C) in direct comparison to the enzyme after treatment with lipase A_2 (B) as well as control experiments including mediators and Tris buffer only (A). All experiments including mediators for a potential step from −0.29 to 0.71 V which contribute to the fully reduced and fully oxidized forms respectively. Despite the complete inactivation of the enzyme electrochemically induced difference spectra of the bc_1 complex after depletion of lipid have been found to be stable and the protein to react reversibly, as controlled by comparing the data at different points of the averaging procedure that takes several hours. For better comparability, the data shown was made on the basis of one preparation.

The direct comparison of the oxidized-minus-reduced FTIR difference spectra of the bc_1 complex with and without lipid reveals strong changes in the full spectral range between 1800 and 850 cm^{-1}.

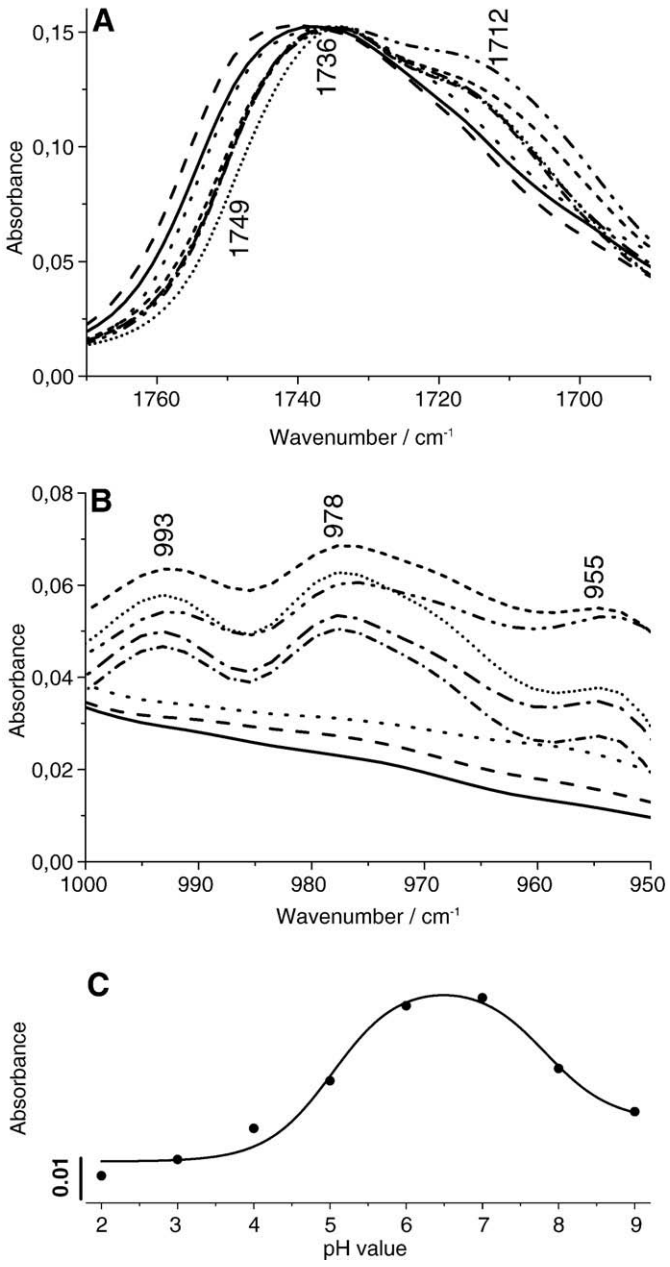

Fig. 3. Enlarged view of the absorbance spectra of cardiolipin at pH 2–pH 9 in steps of 1 pH unit: the pH dependent variation of the ν(C=O) vibration at 1749 and 1712 cm^{-1} (A) as well as the $\nu(PO_3^{2-})$ modes at 993 and 955 cm^{-1} (B) at pH 2 (solid line), pH 3 (dashed line), pH 4 (dotted line), pH 5 (dashed dotted line), pH 6 (dashed dotted dotted line), pH 7 (short dash line), pH 8 (short dot line) and pH 9 (short dash dot line). Spectra C shows the pK_a-values determination for the respective $\nu(PO_3^{2-})$ signal at 955 cm^{-1} and are averaged for the ν(C=O) at 1749 and 1712 cm^{-1} as well as for the $\nu(PO_3^{2-})$ modes at 993, 978 and 955 cm^{-1}. The first pK_a value is found at 4.7 ± 0.3, and for the second protonation is averaged at 7.9 ± 1.3.

These variation include changes in the amide I (1690–1620 cm^{-1}) and amide II (1560–1520 cm^{-1}) range, were contributions from the protein backbone are involved. Interestingly higher signal intensity can be observed, i.e. 1628 and 1531 cm^{-1}. Variation of the heme modes, previously assigned for the wild-type [45,46,60] i.e. around 1550 cm^{-1}, cannot be excluded as well. A major differential feature at app. 1390 cm^{-1} is observable in the spectra in absence of lipid. The spectral range is rather unspecific and a tentative assignment is not possible. The signals involving contributions from the Glu272 side chain at 1734 cm^{-1} [61], however, are not significantly changed, indicating that this spectral range is not influenced by lipids in the studied preparation, as found previously for complex I and Rhodopsin [29,30,33].

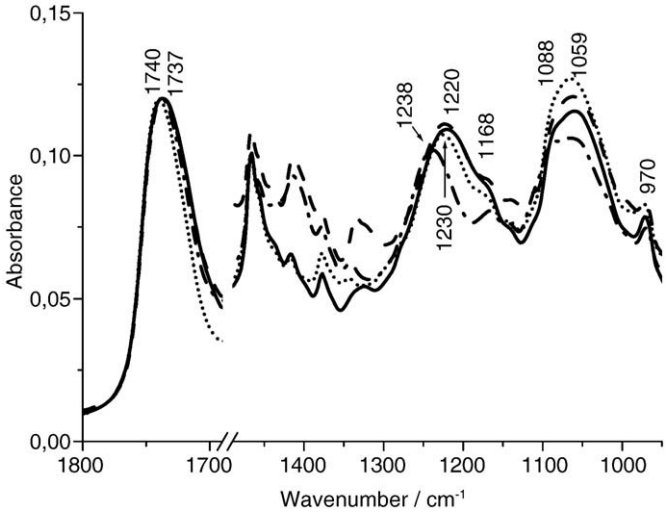

Fig. 4. Infrared absorbance spectra of mixed lipids at selected pH values, pH 2 (solid line), pH 3 (dashed line), pH 5 (dashed dotted line), and pH 8 (dotted line) and pH 9.

In order to highlight the spectral region were the phosphate groups are expected, the enlarged view of the spectral region from 1200 and 900 cm^{-1} (Fig. 6) in direct comparison to the spectra of the protonation of cardiolipin (pH 9–pH 2) as well as the protonation of mixed lipids is presented.

The main variations seen in this spectral region concern the differential feature at 1113, 1159, 1039, 1020 and 980 cm^{-1}. These modes clearly correlate with lipid signals of the head group. We note that the reorganization of the lipids with the redox reaction will induce positive and negative signals in the moment changes of the

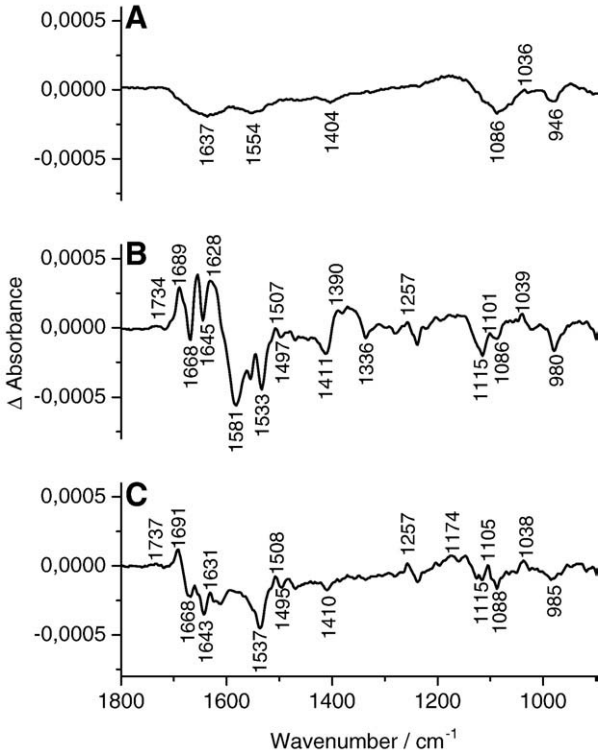

Fig. 5. Oxidized-minus-reduced FTIR difference spectra from Tris buffer (A), the depleted cytochrome bc_1 complex (B) and wild type (C) for a full potential step from −0.29 to 0.71 V shown from 1800 to 950 cm^{-1}.

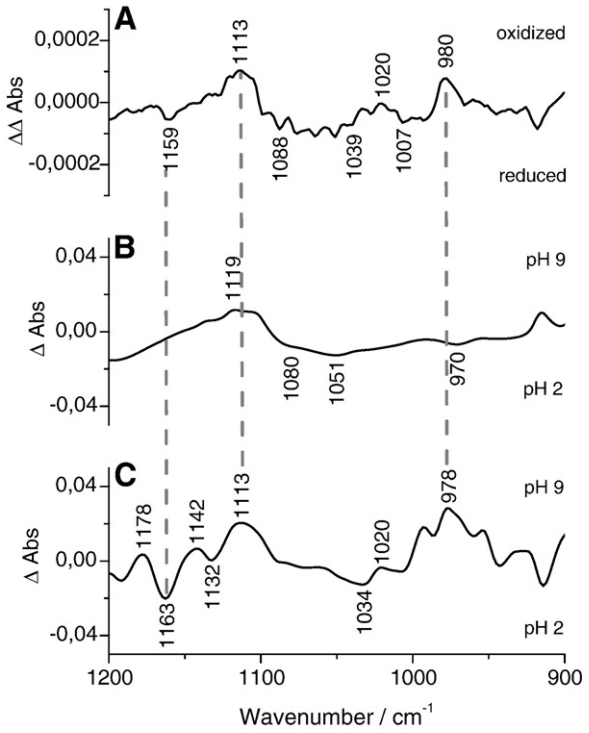

Fig. 6. Enlarged view of the spectral region from 1200 and 900 cm^{-1} (see Fig. 5) as double difference spectra by subtraction the lipid-free bc_1-minus-wildtype spectra (A) in direct comparison to the difference spectra of mixed lipid (B) and cardiolipin vesicle (C) in protonated and deprotonated form by subtraction the absorbance spectra from pH 2–pH 9.

environment occur upon the induced electron transfer and coupled conformational changes or protonation events. Most of the lipids present in the enzyme will thus not be affected and not contribute in the redox induced difference spectra. We cannot exclude, that in addition to the critical cardiolipin molecule discussed, further lipids, move as a indirect response to the electron transfer of the different cofactors. Furthermore contributions from amino acid side chains [4] or hemes are involved here [62,63]. We note that they are expected to be rather small. Most of the signals seen, like the broad band between 1088 and 1039 cm^{-1}, correlate with typical modes of the cardiolipin molecule (Fig. 6C). The difference spectra obtained for the protonation of CL in solution (pH 2–pH 9) display clear similarities with the features lost in the bc_1 complex after delipidation (see Fig. 6A). In contrast the comparison to the spectral features for the protonation of mixed lipids does not show the same degree of similarity. On this basis of the shifts of the head group vibrations at 1159, 1113, 1039 and 980 cm^{-1} the protonation of cardiolipin coupled to the reduction is suggested. Since the contributions of the PO groups are sensitive to the hydrogen-bonding environment, as shown in Fig. 1, some of the spectral features may be due to from the movement of the protein as induced by the redox reaction. The tentative assignments of the bc_1 complex are summarized in Table 2.

3.2.2. Redox induced FTIR difference spectra after addition of cardiolipin

Upon addition of cardiolipin, but not of other lipids, a reactivation of the yeast enzyme is observed [43] as also described for the bovine complex [38]. We have performed redox induced FTIR difference spectra of the enzyme after addition of cardiolipin to the lipase A_2 treated enzyme (Fig. 7B), of asolectin with cardiolipin (C) in direct comparison to the protein in the absence of lipids (A) and wild-type (D). Overall some of the changes induced by lipid depletion change are compensated, however, not all of them. We note that the data obtained with CL alone indicated a rather unstable sample, that changed its spectral properties after several reaction cycles. The addition of asolectin was found to be essential for stabilization.

The major change in the amide I range (1690–1620 cm^{-1}), that possibly reflects a variation of the polypeptide backbone, is only partially compensated. Certainly not all lipid molecules are integrated in their binding sites, but are attached to the protein. The binding site may also contain fragments from the original lipid (or detergent molecules) bound non-specifically to the site; but avoiding the new lipid molecules to accommodate at the site. This is in line with the only partial reactivation. Correspondingly signals arise that correspond to the model compounds studies indicated for example with the signal at 1728 cm^{-1}.

Table 2
Tentative assignments for the electrochemically induced FTIR spectra of the bc_1 complex from yeast with and without lipid and after re-addition of lipids

wt	Lipid depleted	AsoCL addition	Assignments		Ref
1737 (+)	1734 (+)		υ(C=O)	Asp/Glu	a,b,c,f
		1730 (+)	υ(C=O)	Lipid contribution	
1710 (+)	1707 (s)		υ(C=O)	Asp/Glu	a,b,c,f
1691 (+)	1689 (+)	1695 (+)	amide I	(Rieske/β-sheet)	a,b
			υ(C=O)	Heme propionates b_L, b_H	a,b,h
1668 (−)	1668 (−)	1662 (−)	$\upsilon_{as}(CN_3H_5)$	Arg	a,b,c,f
			υ(C=O)	Gln/Asn	f
1660 (+)	1655 (+)	1658 (+)	amide I	α-helical	a,b,c,d,e
			υ(C=O)	Quinone	a,b,c,d,e
1643 (−)	1645 (−)	1645 (−)	amide I		
1631 (+)	1628 (+)	1630 (s)	amide I	(Rieske/β-sheet)	a,b,c,d,e
			υ(C=O)	quinone	a,b,c,d,e
			$\upsilon_s(CN_3H_5)$	Arg	a,b,c,d,e,f
			υ_{37}	Heme c_1	a,b,c,d,e,g
1620 (+)	1620 (s)	1620 (s)	δ (NH_2)	Gln/Asn	a,b,f
1612 (−)			υ(C=C)	Quinone	a,b,e
1595 (+)		1606 (+)	υ_{37}	heme b_L, b_H	a,b
	1581 (−)	1570 (−)			
1574 (+)			amide II		
			$\upsilon_{as}(COO^-)$	Heme propionates b_L, b_H, c_1	a,b,h
1558 (s)	1562 (+)	1558 (s)	υ_{38}	Heme b_L, b_H	a,b
1550 (+)	1545 (+)		υ_{38}	heme c_1	a,b,g
1537 (−)	1533 (−)	1537 (−)	amide II		
			$\upsilon_{as}(COO^-)$	Asp/Glu	a,b,f
			$\upsilon_{as}(COO^-)$	Heme propionates b_L, b_H, c_1	a,b,f,g
1518 (+)	1518 (s)	1518 (s)	$\upsilon_{19}(CC)_{ring}$	Tyr-OH	a,b,f
1508 (+)	1507 (+)	1504 (+)	amide II		
1495 (−)	1497 (−)	1496 (−)		Quinone ring	a,b,e
			$\upsilon_{19}(CC)_{ring}$	Tyr-O^-	a,b,f
1469 (−)	1469 (−)			Quinone ring	a,b
1410 (−)	1411 (−)	1410 (−)		Quinone Ring	a,b
			$\upsilon_s(COO^-)$	Heme propionates b_L, b_H, c_1	a,b,g,h
1371 (+)	1370 (+)	1367 (+)			
1292 (+)	1292 (+)		υ(C–O)	Methoxy group, Quinone	a,b,e
1269 (s)	1267 (s)	1265 (+)	υ(C–O)	Methoxy group, quinone	a,b,e
1257 (+)	1257 (+)		υ_{42}	Heme b_L, b_H, c_1	a,b,g,h
			$\upsilon_7'_a(C–O^-)$	Tyr	a,b,f
1238 (−)	1238 (−)	1240 (−)	δ (COH)	Tyr	a,b,f
1203 (+)	1202 (+)	1203 (+)		Quinone	a,b,e
1174 (+)	1178 (+)	1186 (+)		Lipid contribution	
1159 (−)				Quinone	a,b,e
1147 (+)	1149 (+)	1151 (+)	$(C–C)_{vinyl}$	heme b_L	a,b
1115 (−)	1115 (−)	1116 (−)		Lipid contribution	a,b
1105 (+)	1101 (+)	1103 (+)	$\delta (=CH_2)_{vinyl}$	Heme b_H	a,b
1088 (−)	1086 (−)	1088 (−)	$\upsilon(PO_2^-)$	Lipid contribution, CL	
985 (−)	980 (−)	989 (−)		lipid contribution	

Positions are given in cm^{-1}. Positive signals describing the oxidized state from the enzyme (+), the reduce state (−) and shoulders (s). (Assignments of the cytochrome bc_1 complex are based on Ref. a: Ritter et al. [45], b: Ritter et al. [46], c: Baymann et al. [66], d: Iwaki et al. [5,60,65], e: Hellwig et al. [25], f: Wolpert and Hellwig [4], g: Marboutin et al. [62] h: Berthomieu et al. [64]).

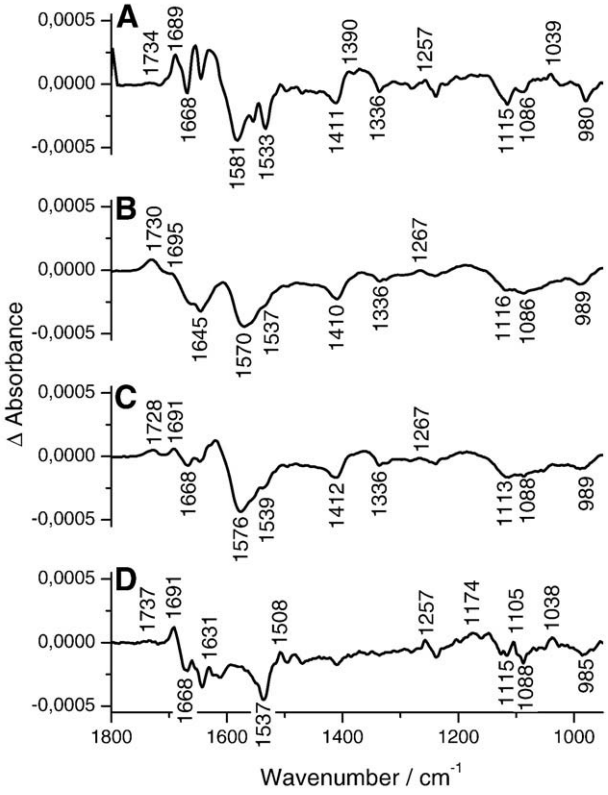

Fig. 7. Oxidized-minus-reduced FTIR difference spectra of the cytochrome bc_1 complex from yeast after addition of cardiolipin (B) and a mix of cardiolipin and asolectin (C) in direct comparison to the protein in the absence of lipid (A) and the wild type as isolated (D). Data were not normalized.

3.3. Electrochemically induced vis difference spectra

All samples studied in infrared have also been analyzed in the visible spectral range. Fig. 8 shows the reduced-minus-oxidized difference spectra in the visible spectral range for the cytochrome bc_1 complex as isolated in direct comparison to the lipid depleted form for the full potential step and for selected potential steps revealing the contributions of each heme.

Clearly a shift of the alpha band from 559 to 556 nm can be seen after depletion of the lipids, indicating influence of the lipids on the hemes *b* and heme *c* spectral properties. The spectra at selected potential steps reveal that the interaction not only concerns the heme b_H as found on the basis of potential titrations with the same method but also heme *c*.

4. Discussion

In this work we demonstrate the possibility to study the functional role of specifically bound lipids in enzymes by means of redox induced FTIR difference spectroscopy. Importantly it could be observed that the presence and absence of lipids, which are not redox active themselves, have a strong influence on the spectral properties.

First vibrational modes sensitive for structural rearrangements and pH dependent shifts, were found on the basis a systematic study of model compounds. The direct comparison of the vesicle and micelle form of the lipids show, that nearly all vibrations are sensitive towards the structural arrangement. Two pK_a values for the vesicle form of cardiolipin could be determined. The first protonation step is found at 4.7 and the second pH dependent change is observed at pH 7.9. Haines and Dencher [59] recently suggested that the relatively high pK_a value for the second protonation event has its origin on the direct interaction between the phosphate group and the OH head group. This ring type structure is certainly not expected in the protein, but it demonstrates the high susceptibility of the pK_a values for strong shifts and it is not clear what to expect for the pK_a value within the protein.

In the case of the bc_1 complex from yeast monitored here, two cardiolipin molecules have been found in X-ray structures, one closely bound to center N [22] close to the quinone binding site and heme b_H and a second one, which is bound in less delipidated samples at the subunit interface of cytochrome *b* and core protein 1 [22,25].

The oxidized-minus-reduced FTIR difference spectra of the cytochrome bc_1 complex at pH 7.3 include marker bands found for the protonated and deprotonated form of cardiolipin and we conclude that the bound lipids are perturbed by the redox reaction. One possible explanation of the data is that cardiolipin is deprotonated in the oxidized state and uptakes a proton in the reduced state of the enzyme. Signals due to the changes in hydrogen bonding environment of the lipids and coupled structural rearrangements are also proposed and will be distinguished in future studies with the help of site-directed mutagenesis and isotope-labeled lipids.

The shift of the heme b_H and heme *c* contribution in the reaction induced visible spectra confirms the importance of the lipids for structural and electrostatic integrity. Finally it could be shown that reaction induced infrared difference spectroscopy is a sensitive tool for the study of the effect of lipids specifically bound to membrane proteins on molecular level. This is in line with data presented for bacteriorhodopsin and complex I for lipids attached to the protein [29,30,33,67]. Preparation dependent variations on lipid content may thus not only change the activity of the respective protein, significant changes in the reaction induced data and thus on the local structure of

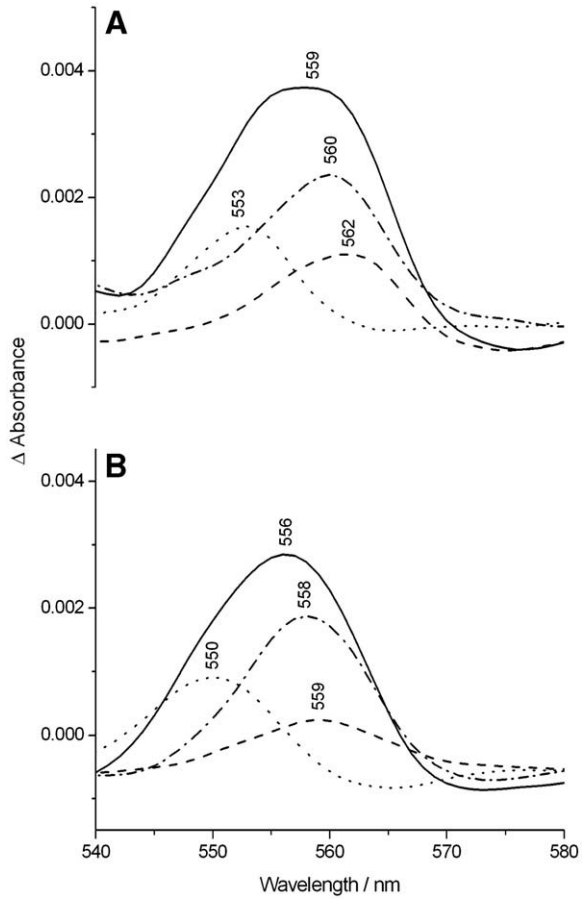

Fig. 8. Reduced-minus-oxidized difference spectra in the visible spectral range for the lipid depleted cytochrome bc_1 complex (B) from yeast at selected potential steps revealing the contributions of each heme in direct comparison to the oxidized-minus-reduced UV–vis difference spectra of the wild type (A).

the cofactors side close to the lipid binding can be concluded. In conclusion, the lipids may be part of the integral structure and participate in the enzymes function.

Acknowledgements

Financial support by DFG SFB 472 the Volkswagen foundation, the CNRS and the Agence National de Recherche is gratefully acknowledged.

References

[1] R. Vogel, F. Siebert, Vibrational spectroscopy as a tool for probing protein function, Curr. Opin. Chem. Biol. 4 (2000) 518–523.
[2] K. Gerwert, Molecular reaction mechanisms of proteins monitored by time-resolved FTIR-spectroscopy, Biol. Chem. 380 (1999) 931–935.
[3] A. Mezzetti, W. Leibl, J. Breton, E. Nabedryk, Photoreduction of the quinone pool in the bacterial photosynthetic membrane: identification of infrared marker bands for quinol formation, FEBS Lett. 537 (2003) 161–165.
[4] M. Wolpert, P. Hellwig, Infrared spectra and molar absorption coefficients of the 20 alpha amino acids in aqueous solutions in the spectral range from 1800 to 500 cm^{-1}, Spectrochim. Acta, A Mol. Biomol. Spectrosc. 64 (2006) 987–1001.
[5] M. Iwaki, G. Yakovlev, J. Hirst, A. Osyczka, P.L. Dutton, D. Marshall, P.R. Rich, Direct observation of redox-linked histidine protonation changes in the iron–sulfur protein of the cytochrome bc1 complex by ATR-FTIR spectroscopy, Biochemistry 44 (2005) 4230–4237.
[6] S. Dörr, M. Wolpert, P. Hellwig, Study on the redox dependent γ (CH) vibrational modes of c-type heme, Biopolymers 82 (2006) 349–352.
[7] S. Dörr, U. Schade, P. Hellwig, Far infrared spectroscopy on hemoproteins: a model compound study from 1800–100 cm (−1), Vibr. Spectrosc. 47 (2008) 59–65.
[8] S. Dörr, U. Schade, P. Hellwig, M. Ortolani, Characterisation of the temperature dependent Fe-imidazol vibrational modes in far infrared, J. Phys. Chem. B-4 111 (2007) 14418–14422.
[9] Y. El Khoury, P. Hellwig, Infrared spectroscopic characterization of copper-polyhistidine from 1,800 to 50 cm (−1): model systems for copper coordination, J. Biol. Inorg. Chem. 14 (1) (2009) 23–34.
[10] D.F. Plusquellic, K. Siegrist, E.J. Heilweil, O. Esenturk, Applications of terahertz spectroscopy in biosystems, Chemphyschem. 8 (2007) 2412–2431.
[11] U. Heugen, G. Schwab, E. Bründermann, M. Heyden, X. Yu, D.M. Leitner, M. Haventith, Solute-induced retardation of water dynamics probed directly by terahertz spectroscopy, Proc. Natl. Acad. Sci. U. S. A. 103 (2006) 12301–12306.
[12] H.H. Mantsch, A. Martin, D.G. Cameron, Characterization by infrared spectroscopy of the bilayer to nonbilayer phase transition of phosphatidylethanolamines, Biochemistry 20 (1981) 3138–3145.
[13] A. Blume, W. Hübner, G. Messner, Fourier transform infrared spectroscopy of ^{13}C=O-labeled phospholipids hydrogen binding to carbonyl Groups, Biochemistry 27 (1988) 8239–8249.
[14] W. Hübner, H.H. Mantsch, M. Kates, Intramolecular hydrogen bonding in cardiolipin, Biochim. Biophys. Acta 1066 (1991) 166–174.
[15] H.H. Mantsch, R.N. McElhaney, Phospholipid phase transitions in model and biological membranes as studied by infrared spectroscopy, Chem. Phys. Lipids 57 (1991) 213–226.
[16] A. Désormeaux, G. Laroche, P.E. Bougis, M. Pezolet, Characterization by infrared spectroscopy of the interaction of a cardiotoxin with phosphatidic acid and with binary mixtures of phosphatidic acid and phosphatidylcholine, Biochemistry 31 (1992) 12173–12182.
[17] A.V. Popova, D.K. Hincha, Intermolecular interations in dry and rehydrated pure and mixed bilayers of phosphatidylcholine and digalactosyldiacylglycerol: a Fourier transform infrared spectroscopy study, Biophys. J. 85 (2003) 1682–1690.
[18] H.L. Casal, I.C. Smith, D.G. Cameron, H.H. Mantsch, Lipid reorganization in biological membranes: a study by Fourier transform infrared difference spectroscopy, Biochim. Biophys. Acta 550 (1979) 145–149.
[19] R. Mendelsohn, G. Anderle, M. Jaworsky, H.H. Mantsch, R.A. Dluhy, Fourier transform infrared spectroscopic studies of lipid–protein interaction in native and reconstituted sarcoplasmic reticulum, Biochim. Biophys. Acta 775 (1984) 215–224.
[20] W.K. Surewicz, T.M. Stepanik, A.G. Szabo, H.H. Mantsch, Lipid-induced changes in the secondary structure of snake venom cardiotoxins, J. Biol. Chem. 263 (1988) 786–790.
[21] K.E. McAuley, P.K. Fyfe, J.P. Ridge, N.W. Isaacs, R.J. Cogdell, M.R. Jones, Structural details of an interaction between cardiolipin and an integral membrane protein, Proc. Natl. Acad. Sci. 96 (1999) 14706–14711.
[22] C. Lange, J.H. Nett, B.L. Trumpower, C. Hunte, Specific roles of protein–phospholipid interactions in the yeast cytochrome bc_1 complex structure, EMBO J. 20 (2001) 6591–6600.
[23] K. Shinzawa-Itoh, H. Aoyama, K. Muramoto, H. Terada, T. Kurauchi, Y. Tadehara, A. Yamasaki, T. Suginura, S. Kurono, K. Tsujimoto, T. Mizushima, E. Yamashita, T. Tsukihara, S. Yoshikawa, Structures and physiological roles of 13 integral lipids of bovine heart cytochrome c oxidase, EMBO J. 26 (2007) 1713–1725.
[24] A.G. Lee, Lipid–protein interactions in biological membranes: a structural perspective, Biochim. Biophys. Acta 1612 (2003) 1–40.
[25] H. Palsdottir, C. Hunte, Lipids in membrane protein structures, Biochim. Biophys. Acta 1666 (2004) 2–18.
[26] C. Hunte, Specific protein–lipid interactions in membrane proteins, Biochem. Soc. Trans. 33 (2005) 938–942.
[27] F. Siebert, W. Mäntele, W. Kreutz, Evidence for the protonation of two internal carboxylic groups during the photocycle of bacteriorhodopsin: investigation by kinetic infrared spectroscopy, FEBS Lett. 141 (1982) 82–87.
[28] M. Engelhard, K. Gerwert, B. Hess, W. Kreutz, F. Siebert, Light-driven protonation changes of internal aspartic acids of bacteriorhodopsin: an investigation of static and time-resolved infrared difference spectroscopy using [4-^{13}C] aspartic acid labeled purple membrane, Biochemistry 24 (1985) 400–407.
[29] M. Beck, F. Siebert, T.P. Sakmar, Evidence for the specific interaction of a lipid molecule with rhodopsin which is altered in the transition to the active state metarhodopsin II, FEBS Lett. 436 (1998) 304–308.
[30] J. Isele, T.P. Sakmar, F. Siebert, Rhodopsin activation affects the environment of specific neighboring phospholipids: an FTIR spectroscopic study, Biophys. J. 79 (6) (2000) 3063–3071.
[31] P. Hellwig, D. Scheide, S. Bungert, W. Mäntele, T. Friedrich, FT-IR spectroscopic characterization of NADH:ubiquinone oxidoreductase (complex I) from *Escherichia coli*: oxidation of FeS cluster N2 is coupled with the protonation of an aspartate or glutamate side chain, Biochemistry 39 (2000) 10884–10891.
[32] P. Hellwig, S. Stolpe, T. Friedrich, Fourier transform infrared spectroscopic study on the conformational reorganization in *Escherichia coli* complex I due to redox-driven proton translocation, Biopolymers 74 (2004) 69–72.
[33] R. Hielscher, T. Wenz, S. Stolpe, C. Hunte, T. Friedrich, P. Hellwig, Monitoring redox-dependent contribution of lipids in Fourier transform infrared difference spectra of complex I from *Escherichia coli*, Biopolymers 82 (4) (2006) 291–294.
[34] P. Mitchell, Possible molecular mechanisms of the protonmotive function of cytochrome systems, J. Theor. Biol. 62 (1976) 327–367.
[35] A.B. Berry, M. Guergova-Kuras, L. Huang, A.R. Crofts, Structure and function of cytochrome *bc* complexes, Annu. Rev. Biochem. 69 (2000) 1005–1075.
[36] S. Iwata, J.W. Lee, K. Okada, J.K. Lee, M. Iwata, B. Rasmussen, T.A. Link, S. Ramaswamy, B.K. Jap, Complete structure of the 11-subunit bovine mitochondrial cytochrome bc_1 complex, Science 281 (1998) 64–71.
[37] Z. Zhang, L. Huang, V.M. Shulmeister, Y. Chi, K.K. Kim, L.W. Hung, A.R. Crofts, E.A. Berry, S.H. Kim, Electron transfer by domain movement in cytochrome bc_1, Nature 392 (1998) 677–684.
[38] B. Gomez Jr., N.C. Robinson, Phospholipase digestion of bound cardiolipin reversibly inactivates bovine cytochrome bc_1, Biochemistry 38 (28) (1999) 9031–9038.
[39] D.A. Six, E.A. Dennis, The expanding superfamily of phospholipase A_2 enzymes: classification and characterization, Biochim. Biophys. Acta 1488 (2000) 1–19.
[40] B. Gomez Jr., N.C. Robinson, Quantitative determination of cardiolipin in mitochondrial electron transferring complexes by silicic acid high-performance liquid chromatography, Anal. Biochem. 267 (1) (1999) 212–216.
[41] C. Hunte, J. Koepke, C. Lange, T. Ro, manith, H. Michel, Structure at 2.3 Å resolution of the cytochrome *bc*(1) complex from the yeast *Saccharomyces cerevisiae* co-crystallized with an antibody F_v fragment, Structure 8 (2000) 669–684.
[42] H. Palsdottir, C. Hunte, Purification of the cytochrome bc_1 complex from yeast, in: C. Hunte, G. von Jagow, H. Schägger (Eds.), Membrane Protein Purification and Crystallization 2/e: A Practical Guide, Elsevier Science, USA, 2003, pp. 191–203.
[43] T. Wenz, R. Hielscher, P. Hellwig, H. Schägger, S. Richers, C. Hunte, Role of phospholipids in respiratory cytochrome bc_1 complex catalysis and supercomplex formation, Biochim. Biophys. Acta 1787 (2009) 609–616.
[44] D.A. Moss, E. Nabedryk, J. Breton, W. Mäntele, Redox-linked conformational changes in proteins detected by a combination of infrared spectroscopy and protein electrochemistry. Evaluation of the technique with cytochrome *c*, Eur. J. Biochem. 187 (1990) 565–572.
[45] M. Ritter, O. Anderka, B. Ludwig, W. Mäntele, P. Hellwig, Electrochemical and FTIR spectroscopic characterization of the cytochrome bc_1 complex from *Paracoccus denitrificans*: evidence for protonation reactions coupled to quinone binding, Biochemistry 42 (2003) 12391–12399.
[46] M. Ritter, H. Palsdottir, M. Abe, W. Mäntele, C. Hunte, H. Miyoshi, P. Hellwig, Direct Evidence fort he interaction of stigmatellin with a protonated acidic group in the bc_1 complex from *Saccharomyces cerevisiae* as monitored by FTIR difference spectroscopy and ^{13}C specific labeling, Biochemistry 43 (2004) 8439–8446.
[47] R.N. Lewis, R.N. McElhaney, W. Pohle, H.H. Mantsch, Components of the carbonyl stretching band in the infrared spectra of hydrated 1,2-diacylglycerolipid bilayers: a reevaluation, Biophys. J. 67 (6) (1994) 2367–2375.
[48] R.N. Lewis, R.N. McElhaney, Fourier transform infrared spectroscopy in the study of hydrated lipids and lipid bilayer membranes, in: H.H. Mantsch, D. Chapman (Eds.), Infrared Spectroscopy of Biomolecules, Wiley-Liss, New York, 1996, pp. 159–202.
[49] S.F. Bush, H. Levin, I.W. Levin, Cholesterol–lipid interactions: an infrared and Raman spectroscopic study of the carbonyl stretching mode region of 1,2-dipalmitoyl phosphatidylcholine bilayers, Chem. Phys. Lipids 27 (1980) 101–111.
[50] R.G. Snyder, Vibrational spectra of crystalline n-paraffins. Part I. Methylene rocking and wagging modes, J. Mol. Spectrosc. 4 (1960) 411–434.
[51] R.G. Snyder, J.H. Schachtschneider, Vibrational analysis of the n-paraffins—I Assignments of infrared bands in the spectra of C_3H_8 through n-$C_{19}H_{40}$, Spectroschim. Acta 19 (1963) 85–116.
[52] R.G. Snyder, M. Maroncelli, H.L. Strauss, V.M. Hallmark, Temperature and phase behavior of infrared intensities: the poly(methylene) chain, J. Phys. Chem. 90 (1986) 5623–5630.
[53] L. Senak, D. Moore, R. Mendelsohn, CH_2 wagging progessions as IR probes of slightly disordered phospholipid acyl chain state, J. Phys. Chem. 96 (1992) 2749–2754.

[54] Y. Guan, C.J. Wurrey, G.J. Thomas Jr., Vibrational analysis of nucleic acids. I. The phosphodiester group in dimethyl phosphate model compounds: $(CH_3O)_2PO_2^-$, $(CD_3O)_2PO_2^-$, and $(^{13}CH_3O)_2PO_2^-$, Biophys. J. 66 (1) (1994) 225–235.
[55] M. Klähn, G. Mathias, C. Kötting, M. Nonella, J. Schlitter, K. Gerwert, P. Tavan, IR spectra of phosphate ions in aqueous solution: predictions of a DFT/MM approach compared with observations, J. Phys. Chem. A 108 (2004) 6186–6194.
[56] J.H. Crowe, L.M. Crowe, D. Chapman, Infrared spectroscopic studies on interactions of water and carbohydrates with a biological membrane, Arch. Biochem. Biophys. 232 (1984) 400–407.
[57] H.L. Casal, H.H. Mantsch, H. Hauser, Infrared studies of fully hydrated saturated phosphatidylserine bilayers. Effect of Li^+ and Ca^{2+}, Biochemistry 26 (1987) 4408–4416.
[58] M. Kates, J.Y. Syz, D. Gosser, T.H. Haines, pH-dissociation characteristics of cardiolipin and its 2′-deoxy analogue, Lipids 28 (1993) 877–882.
[59] T.H. Haines, N.A. Dencher, Cardiolipin: a proton trap for oxidative phosphorylation, FEBS Lett. 528 (2002) 35–39.
[60] M. Iwaki, L. Giotta, A.O. Akinsiku, H. Schägger, N. Fisher, J. Breton, P.R. Rich, Redox-induced transitions in bovine cytochrome bc_1 complex studied by perfusion-induced ATR-FTIR spectroscopy, Biochemistry 42 (2003) 11109–11119.
[61] T. Wenz, P. Hellwig, F. MacMillan, B. Meunier, C. Hunte, Probing the role of E272 in quinol oxidation of mitochondrial complex III, Biochemistry 45 (2006) 9042–9052.
[62] L. Marboutin, A. Boussac, C. Berthomieu, Redox infrared markers of the heme and axial ligands in microperoxidase: bases for the analysis of *c*-type cytochromes, J. Biol. Inorg. Chem. 11 (2006) 811–823.
[63] S. Choi, T.G. Spiro, K.C. Langry, K.M. Smith, D.L. Budd, G.N. La Mar, Structural correlations and vinyl influences in resonance Raman spectra of protoheme complexes and proteins, J. Am. Chem. Soc. 104 (1982) 4345–4357.
[64] C. Berthomieu, A. Boussac, W. Mäntele, J. Breton, E. Nabedryk, Molecular changes following oxidoreduction of cytochrome b_{559} characterized by Fourier transform infrared difference spectroscopy and electron paramagnetic resonance: photo-oxidation in photosystem II and electrochemistry of isolated Cytochrome b_{559} and iron protoporphyrin IX-bisimidazole model compounds, Biochemistry 31 (1992) 11460–11471.
[65] M. Iwaki, A. Osyczka, C.C. Moser, P.L. Dutton, P.R. Rich, ATR-FTIR spectroscopy studies of iron–sulfur protein and cytochrome c_1 in the *Rhodobacter capsulatus* cytochrome bc_1 complex, Biochemistry 43 (2004) 9477–9486.
[66] F. Baymann, D.E. Robertson, P.L. Dutton, W. Mäntele, Electrochemical and spectroscopic investigations of the cytochrome bc_1 complex from *Rhodobacter capsulatus*, Biochemistry 38 (1999) 13188–13199.
[67] L. Sinegina, M. Wikstrom, M.I. Verkhovsky, M.L. Verkhovskaya, Activation of isolated NADH:ubiquinone reductase I (complex I) from *Escherichia coli* by detergent and phospholipids. Recovery of ubiquinone reductase activity and changes in EPR signals of iron–sulfur clusters, Biochemistry 44 (23) (2005) 8500–8506.